

# An Improved Connectivity based Outlier Factor Median Filter (ICOFMED)

Bello, Baththama Alhassan  
Department of Computer Science  
Ahmadu Bello University, Zaria  
bbal hassan8510@gmail.com

M.A Bagiwa  
Department of Computer Science  
Ahmadu Bello University, Zaria  
Mstphaminu@yahoo.com

A. F. Donfack Kana  
Department of Computer Science  
Ahmadu Bello University, Zaria  
dkana@abu.edu.ng

Muhammad Abdullahi  
Department of Computer Science  
Ahmadu Bello University, Zaria  
Muham08@gmail.com

**Abstract**— Salt-and-pepper (SAP) noise is a common issue caused by abrupt and sharp disturbances in the image signal caused by Transmission Errors, Sensor Malfunctions, leading to a significant decline in image quality. While considerable advancements have been achieved in removing salt-and-pepper noise, the challenge of image blurring and distortion persists. There is a need to enhance the efficiency of denoising techniques. This paper proposed an enhanced switching method for detecting and removing salt-and-pepper noise using an improved Connectivity-Based Outlier Factor (COF) algorithm. The approach involves two main steps: firstly, employing the enhanced COF to accurately identify noise pixels, and secondly, applying a median filter to these noisy pixels for noise removal. The experimental results show that the Improved Connectivity-Based Outlier Factor (ICOFMed) technique performs well across a wide range of noise densities, as measured by subjective visual and objective digital evaluations. However, as noise levels increase, for example, to 50%, the capacity to recover image quality decreases, as indicated by diminishing PSNR and SSIM values for highly noisy images. While the recommended technique is beneficial, the paper indicated possible areas for improvement(s).

**Keywords**—denoising, Salt and pepper, COF, median filter

## I. INTRODUCTION

This Images affected by noise suffer from a loss of visual appeal as they can either remove or add details to the original scenes they represent. Among various types of noise, salt-and-pepper noise (SAP) is a common occurrence in images due to factors like faulty channels during image transmission or defective image sensors while capturing pictures [3]. SAP, categorized as impulse noise, consists of pixels with extreme intensity (maximum or minimum) that often stand out from the surrounding noise-free pixels, causing them to appear as either white or black pixels in the corrupted image [10]. Even at low noise densities, SAP can significantly degrade visual quality and hinder image analysis, necessitating its detection and removal [2]. In fact, it would be especially beneficial to keep improving denoising algorithms when the noise density of the images is low. While the focus has often been on addressing high-density noise, the ability to efficiently restore and improve images with low-level noise can greatly increase the usefulness of these methods. The difficulty in restoring image details becomes more challenging when dealing with heavy salt-and-pepper noise, leading to substantial information loss. Consequently, noise removal becomes essential before further processing of such images.

Certainly, significant progress has been achieved in reducing the presence of salt and pepper noise in digital images. But the persistent problems with image distortion and blurring highlight the continuous need to improve and hone denoising methods.

These difficulties pose significant roadblocks to the creation of cleaner, higher-quality images, necessitating creative methods to increase denoising procedures' overall effectiveness. Not only do developments in this subject help the image processing industry, but they also have great potential for use in a variety of applications where image integrity and clarity are crucial, such as computer vision systems, surveillance, and medical imaging.

Spatial domain techniques are based on operating on individual pixels or groups of pixels directly using a window of a specified size. Switching median filters were introduced as a solution to the blurring issues caused by classical filters and their variations, which replaced every pixel in the image, regardless of whether it was noisy or not. To overcome the blurring issues of classical filters, these filters perform noise identification prior to filtering. They first categorize each pixel as either corrupted or uncorrupted based on some criteria, and then only the corrupted pixels are replaced. It has already been established that detection methods have an impact on the level of performance of any noise reduction scheme. The better the detection, the better the outcome. As a result, the performance of the detector is critical.

The performance of image denoising filters depends on several factors, including the type and level of noise present in the image, the filter's parameters, and the size of the filter's processing window. In general, the ideal denoising filter should strike a balance between noise reduction and detail preservation, ensuring that the image remains visually appealing and suitable for further analysis or processing tasks.

Outlier detection method is essential in removing noise from noisy images. The technique of discovering pieces of data or points that are dissimilar to other items or expected pattern in a dataset is known as outlier detection [1]. Statistical methods, proximity-based methods, and clustering-based methods are the three most common types of outlier detection methods [1][8]. Distance-based and density-based outlier detection methods are the two types of proximity-based outlier detection methods. The connectivity-based outlier factor (COF) is a density-based strategy for identifying outliers. It is a refined version of the local outlier factor (LOF) technique, except that the density estimation of the COF for the data points is done differently by a different method termed the chaining distance while the KNN in the LOF is calculated using the Euclidean distance. The Connectivity-based Outlier Algorithm assigns a degree of Outlyingness to each data point. This degree of Outlyingness is referred to as the data point's connectivity-based outlier factor (COF). A data point with a high COF value is more likely to be an outlier.

Evaluating the performance of denoising filters often involves using objective metrics (such as peak signal-to-noise ratio, mean squared error) and subjective visual inspection to compare the denoised images with the original noise-free images. Researchers continue to develop advanced denoising algorithms to achieve better performance under different noise conditions and improve the overall quality of denoised images. The median filters are useful for smoothing noise and retaining edges

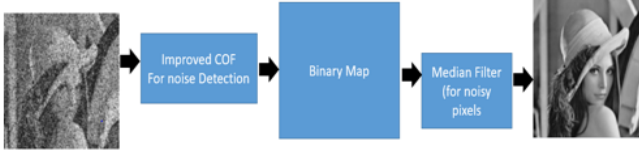


Figure 1: Stages of ICOFMED

This paper introduces an improved version of COF for detecting noisy pixels in a corrupted image  $C$  affected by impulse noise. The proposed method consists of two stages: the first is the noise detection stage, where COF plays a fundamental role in the detection stage, and finally, the image denoising stage. Figure 1 illustrates these stages. During the noise detection stage, each pixel in the corrupted image  $C$  is classified as either noisy or noise-free, and this information is stored in a binary map known as the noise mask  $N$ . In the image denoising stage, the pixels identified as noisy in the noise mask  $N$  undergo a process to estimate their original intensity values. The resulting restored image is denoted as  $R$ .

The rest of the study is organized as follows: In Section II, the introduction of SPN and various important concepts related to it is provided. Section III, Related works section IV new method called "Improved Connectivity-Based Median Filter (ICOFMed)" is discussed. The experimental data and their analysis are presented in Section V. Lastly, the research concludes with Section VI and section VII recommendation.

## II. PRELIMINARIES AND NOTIONS

This section provides some basic notions.

Definition 2.1 describes the dynamic range of pixel intensity values (pixel values)  $[ \alpha \min, \alpha \max ]$ , i.e.  $\alpha \min \leq u_{ij} \leq \alpha \max$ .

Therefore, the corrupted image is represented by:

$$C_{ij} = \begin{cases} \alpha \min & \text{with probability } p \\ \alpha \max & \text{with probability } q \\ C_{ij} & \text{with probability } 1 - q + p \end{cases}$$

Definition 2.2:  $U := [u_{ij}] m \times n$  defines an image matrix (I) where  $u_{ij}$  is an unsigned integer number and  $0 \leq u_{ij} \leq 255$ .

Definition 2.3:  $U := [u_{ij}] m \times n$  be an IM,  $u_{ij}$  is called a noisy pixel intensity value of  $U$  if  $u_{ij} = 0$  or  $u_{ij} = 255$ ; otherwise,  $u_{ij}$  is called a non-noisy entry of  $A$ .

Definition 2.4: Let  $N$  be an Image matrix, if some  $i$  and  $j$ ,  $u_{ij}$  is a noisy value of  $U$ . Then,  $U$  is called a noise image matrix (NIM),

Definition 2.5: Let  $N$  be a corrupted IM. Then,  $B := [b_{ij}] m \times n$  is called binary matrix of  $A$  where  $b_{ij} = \{0, 1, a_{ij}$  is a noisy entry of  $A$  otherwise

Definition 2.6:  $\text{dist}(P, Q) = \min\{\text{dist}(x, y) : x \in P \text{ \& } y \in Q\}$ , and call  $\text{dist}(P, Q)$  the distance between  $P$  and  $Q$ . For any given  $q \in Q$ , we say that  $q$  is the nearest neighbour of  $P$  in  $Q$  if there is a  $p \in P$  such that  $\text{dist}(p, q) = \text{dist}(P, Q)$ . Where  $P, Q \subseteq D, P \cap Q = \emptyset$  and  $P, Q = \emptyset$ .

**Salt and Pepper Noise (SPIN):** The salt-and-pepper noise is also called as impulse or spike noise. This type of noise can be caused by analog-to-digital converter errors, bit errors in transmission, etc. An image with impulse noise will have dark pixels in bright regions and bright pixels in dark regions.

Noises corrupt the digital images during their acquisition, transmission and processing. Images are acquired using the image sensors, and the performance of imaging sensors is affected by factors such as quality of sensing elements, environmental conditions during image acquisition, knowledge and expertise of the person, etc. For example, sensor temperature and lighting levels affect the noise level in images acquired using CCD cameras and the interference in transmission channels corrupt the images during their transmission.

**Connectivity-based Outlier Factor:** is an outlier detection technique where LOF (local outlier factor) technique was improved. With COF, all outliers are detected, globally as well as locally, thus making it more effective [9],[17]. In a connectivity-based outlier algorithm, Data points are graded based on their degree of outlier in connectivity-based outlier algorithms. This degree of outlier is called connectivity-based outlier factor; COF of the data point. The high COF value of data point represent the high probability of being an outlier. In datasets where local density and connectivity structure are relevant, the COF algorithm is beneficial for detecting outliers. In this way, outliers (which are more likely to occur when data points are isolated) can be distinguished from data points that are well-connected (which are less likely to occur when data points are isolated).

## III. RELATED WORK

In the work of [5] the first stage of the method determines the distance between the local pixels in a kernel by determining whether the pixels follow a set of rules. The second phase detects the noisy pixel using the distance (threshold); if the pixel is found to be noise, then it is replaced in the processing window with the median value of the neighbouring pixels. If the processing window lacks sufficient informative elements (pixels), the approach of the self-adaptive windowing mechanism is used to set the size of the processing kernel and replace the processing pixel with the processing window's median value, with the process being repeated. This method takes into account the likelihood, which is very useful because it diagnoses the pixel based on its surroundings.

The work of [13] is a two-step method, in the first stage which is the detection stage each pixel is evaluated if the pixel value is 0 or 255 it is considered noise else it is noise free. The second stage is the filtration stage where the Adaptive Unsymmetric Trimmed Shock Filter is used to replace the current noisy pixel. Only three test images were considered with

noise density from 10-96%, the method performed better than the competing methods. However, its computational time is high due to iteration of the shock filter

In [3] pixels having a high intensity and a significant deviation from the mean of neighbouring pixels are considered noisy during the noise detection stage. The noise filtration process utilizes the intensity of one neighbouring noise free pixel, which is closest to the mean of neighbour noise free pixels. When it comes to noise reduction while preserving structural details, the IDF surpasses the competing filters in performance. Nevertheless, due to iterative nature, IDF requires longer processing time.

In the work of [4] the centre pixel of the window is considered noisy if its grey value is equal to the maximum or the minimum value; otherwise, it is a noise-free pixel. If the centre pixel is noisy and then the eps-mean of the non-noisy pixels in the window is assigned as its new grey value. to evaluate this method the cameraman, Lena, TESTIMAGES dataset and the BSDS dataset were used with noise density from 20-80%, it showed IAWMF performed better than the competing methods and the visual quality was good without additional artefacts

The work of [6] presented a four-step denoising approach in which two trimmed median filters (TMF) with window sizes of  $3 \times 3$  and  $5 \times 5$  was employed to estimate noisy pixels in the first stage, namely TMF3 and TMF5. This stage delivers good results for low noise density since these TMFs compute the value of candidate noisy pixel using original (noise-free) pixels and leave this noisy pixel unmodified. TMF5 is utilized in the second stage, which significantly decreases extreme pixels but when noise concentrations are really high, the resulting image may still have remaining noisy pixels. The Adaptive Running Average (ARA) was utilized in denoising these pixels. Finally, the corrupted pixels found on the side-line were filtered by the BPD procedure.

In [7] detection of noisy pixels is done by utilizing a noise detection algorithm named fuzzy morphological alternate filters to identify whether pixels are corrupted or not, then in second stage, the noisy pixels are filtered based on the median of the greatest repeating pixel values, using a window that gradually expands until at least a weak original pixel exist in the considered window, The UC-Berkeley dataset was tested with noise density ranging from 10 to 95 percent, and it was also compared to numerous approaches, showing good results in most cases. However, at high noise densities, this method's performance was compromised.

The work of [2] A triple-stage filter that detects corrupted pixels by pixel value and distribution characteristics in the first stage, in the second stage denoising is done using weighted mean filter applied to the noisy pixels using a dynamic shape symmetrical window with improved detail preservation. Filtering is done in an iteratively in the last stage to minimize artefacts in high noise density. A good number of pictures with 100 natural images from the Berkeley dataset were tested, demonstrating that IWMF outperformed other state-of-the-art filters at various noise densities in both visual quality and objective digital measures. This method is extremely fast in execution speed making it ideal for real-time processing.

In [15] during the stage of detection, If the grey value of the window's centre pixel is an extreme value, it is deemed a noisy candidate, and a window with adaptive size is used to confirm it.

For these potentially noisy pixels, the proportion of pixels in the window with the same candidate value is determined, and then the data is filtered using a threshold, If it is smaller than the threshold, the candidate is regarded as a noisy pixel, otherwise it is noiseless. In the stage of SAP noise elimination, the noisy pixel will be replaced by the mean of its neighbouring pixels. Then we use a SAP noise based nonlocal mean filter to further restore it. NAMF performed better than the competing systems with a good processing system.

For denoising salt and pepper noise [11] proposed a two-stage filter. After lowering the noise in the first stage by utilizing the median of the weakly original pixels to decrease the high-density noise in the second stage. The second stage is used to reduce any remaining noise by employing a dynamic window that gradually enlarges until there is at least a weak origin pixel in the window using the median of the maximum repeating pixel values. The system was tested using UC-Berkeley datasets with noise densities ranging from 10% to 95%. The system was also put up against other systems and outscored them all, however, the visual quality deteriorated when the noise density was high.

In [12] the detection proposed algorithm initially checks for the outliers in a  $3 \times 3$  neighbourhood. If the processed pixel is noisy then check for the presence of noisy pixels with the 4 neighbours; If the 4 neighbours are found to hold outliers, then mean of the 4 neighbours will replace the output. If the 4 neighbours are not noisy then the output is replaced by asymmetrically trimmed Modified Trimean. If all the pixels of the current processing window are noisy then the mean of all elements will replace the processed pixel. If the processed pixel does not hold the outlier, then the pixel is termed as not noisy and left unaltered. The proposed algorithm exhibits excellent noise elimination capability with enhanced edge preservation capability. The algorithm was tested on a standard database and the results of the proposed algorithm were compared to 16 standard and existing algorithms. The proposed algorithm exhibits excellent results in terms of both Quantitative and qualitative measures.

This is also another two-stage approach in [16] firstly, an appropriate AMF will be applied to the noisy image and used to detect the position of noisy pixels. Then a proposed SAP noise removal scheme based on graph signal reconstruction technique is used to denoise the noisy pixels. Experimental results demonstrate that the proposed algorithm performs better when compared to the state-of-the-art methods

#### IV. SCHEME OF THE TWO-STEP ICOFMED FILTER

In this section a two-step SAP noise reduction algorithm called Improved Connectivity based Outlier Factor Median Filter (ICOFMed) is described in depth, a block diagram describing the proposed filter is approach is shown in Figure 1, followed by its algorithm and an illustration using an example.

A). Two images are loaded, one is a clean image and the other representing a noisy image.

B). The quality of the images is evaluated the by calculating the Peak Signal-to-Noise Ratio (PSNR) and the Structural Similarity Index (SSIM) between the clean and noisy images. This gives an insight of the filtering method.

C). Applies a detection operation to the noisy image to detect noisy pixels. The noise detector used in this work is based on a Connectivity Based outlier Factor (COF) approach. It calculates the COF values for each pixel in the image and uses certain criteria (the center pixel value, COF value, and threshold) to decide whether to mark a pixel as noisy or not.

D). The COF outlier detection was improved to used Manhattan distance metrics instead of Euclidean distance and Applies an Isolation Forest (IForest) algorithm for anomaly detection on the COF values. The IForest is used to identify outliers or anomalies in the COF values.

E). Calculates a noise map based on the predicted labels from the IForest. The noise map is a binary image where noisy pixels are marked as 1 and non-noisy pixels are marked as 0.

To accomplish this objective, all the pixels are checked using a pre-defined window of  $3 \times 3$  of that centers on the considered pixel, 8 neighbors and a threshold of 0.2, pixels with COF values greater than 1 are classified as noisy, and pixels with COF values less than or equal to 0.2 are classified as clean.

F). The filtering operation is performed in a loop for each noisy pixel in the image using median filter.

G). Computes the PSNR and SSIM between the original clean image and the filtered image to evaluate the quality of the denoised result.

H). Finally, it displays the clean image, noisy image, and the filtered image along with their titles for visual inspection.

In the initial stage of detection, the improved connectivity-based-outlier factor was used to process the corrupted image. Then, in the second phase, a median filter is employed to reduce the error of the median-type filter,

## V. RESULTS AND DISCUSSIONS

### A). Image Dataset

Some of the Set12 collection of 12 grayscale scenes were used, the images are of  $256 \times 256$  images were used for each test to verify the viability of the proposed method. Noise levels varying from 10 to 50 were considered

### B). Image Quality Assessment Metrics

To check how closely related the denoised image is to the original image, there exist a number of image quality metrics. The most widely used metrics for evaluating the whole reference image quality are the Peak signal-to-noise ratio (PSNR) and the Structure Similarity (SSIM) [14], [11]. Higher PSNR values are required. Structural Similarity (SSIM) was also considered, the SSIM values range between 0 and 1, and 1 means perfect match of the reconstruct image with original one. The definition of the two metrics can be described in equation (1) and equation (2).

$$PSNR(O, R) = 10 \log_{10} \frac{255^2}{\sum_{M, N} \sum_{i=1}^M \sum_{j=1}^N (O(i, j) - R(i, j))^2} \quad (1)$$

$$SSIM(O, R) = [l(o, f)]^\alpha \cdot [c(o, f)]^\beta \cdot [v(o, f)]^\gamma = \frac{(2\bar{a}_O \bar{a}_f + C1)(2\sigma_{of} + C2)}{(\bar{a}_{O^2} + \bar{a}_f^2 + C1)(\sigma_{O^2} + \sigma_f^2 + C2)} \quad (2)$$

$$l(O, R) = \frac{2\bar{a}_O \bar{a}_f + C1}{\bar{a}_O^2 + \bar{a}_f^2 + C1} \quad (3)$$

$$c(O, R) = \frac{2\sigma_{of} + C2}{\sigma_{O^2} + \sigma_f^2 + C2} \quad (4)$$

$$v(O, R) = \frac{\sigma_{of} + C3}{\sigma_O \sigma_f + C3} \quad (5)$$

O, R and denote the Original, reconstructed and corrupted images, with a given size of (M, N), C1, C2 and C3 are represented as constants.

TABLE1 SETUP PARAMETERS

| Component | Parameter                | Value of parameter         |
|-----------|--------------------------|----------------------------|
| Image     | Image Size               | 256x256 pixel              |
|           | Type                     | Grey Scale                 |
| Noise     | Type                     | Impulse                    |
|           | Density of impulse noise | 0.1-0.5<br>Step size = 0.1 |
| Processor | Type                     | i5-64 bit                  |
|           | RAM                      |                            |
|           | Speed                    |                            |
| Metric(s) | PNSR and SSIM            |                            |
| Platform  | Kaggle                   |                            |
| Software  | Python                   |                            |

A visual comparison between the original, the noisy image and de-noised images can be done during the qualitative analysis.

TABLE 2: PNSR AND SSIM VALUES FOR LENA.BMP IMAGE

| Image Name |        | Lena           |       |                |      |
|------------|--------|----------------|-------|----------------|------|
|            | Salt % | Initial (PNSR) | PNSR  | Initial (SSIM) | SSIM |
| 10         | 50     | 15.73          | 30.98 | 0.26           | 0.92 |
| 20         | 50     | 12.87          | 28.45 | 0.15           | 0.89 |
| 30         | 50     | 11.35          | 25.24 | 0.11           | 0.81 |
| 40         | 50     | 10.26          | 21.43 | 0.08           | 0.66 |
| 50         | 50     | 9.56           | 9.56  | 0.07           | 0.50 |

TABLE 3: PNSR AND SSIM VALUES FOR TULIP.PNG IMAGE

| Image Name |    | Tulip.png      |       |                |      |
|------------|----|----------------|-------|----------------|------|
|            |    | Initial (PNSR) | PNSR  | Initial (SSIM) | SSIM |
| 10         | 50 | 15.27          | 28.81 | 0.39           | 0.91 |
| 20         | 50 | 12.44          | 26.44 | 0.24           | 0.87 |
| 30         | 50 | 10.96          | 23.85 | 0.18           | 0.81 |
| 40         | 50 | 9.91           | 20.68 | 0.14           | 0.71 |
| 50         | 50 | 9.18           | 18.31 | 0.11           | 0.59 |

TABLE 4: PSNR AND SSIM VALUES FOR CAMERAMAN.TIF IMAGE

| Image Name |           | Cameraman.Tif  |       |                |      |
|------------|-----------|----------------|-------|----------------|------|
|            |           | Initial (PNSR) | PNSR  | Initial (SSIM) | SSIM |
| <b>10</b>  | <b>50</b> | 15.36          | 26.23 | 0.26           | 0.87 |
| <b>20</b>  | <b>50</b> | 12.44          | 24.84 | 0.16           | 0.83 |
| <b>30</b>  | <b>50</b> | 10.98          | 22.59 | 0.12           | 0.75 |
| <b>40</b>  | <b>50</b> | 9.96           | 20.29 | 0.09           | 0.63 |
| <b>50</b>  | <b>50</b> | 9.21           | 17.90 | 0.08           | 0.49 |

TABLE 5: PSNR AND SSIM VALUES FOR BLACKCAR. IMAGE

| Image Name |           | Blackcar     |       |              |      |
|------------|-----------|--------------|-------|--------------|------|
|            |           | Initial PNSR | PNSR  | Initial SSIM | SSIM |
| <b>10</b>  | <b>50</b> | 14.62        | 24.76 | 0.43         | 0.86 |
| <b>20</b>  | <b>50</b> | 11.73        | 23.11 | 0.29         | 0.83 |
| <b>30</b>  | <b>50</b> | 10.21        | 20.78 | 0.22         | 0.76 |
| <b>40</b>  | <b>50</b> | 9.22         | 18.59 | 0.18         | 0.68 |
| <b>50</b>  | <b>50</b> | 8.43         | 16.59 | 0.15         | 0.58 |

The tables show the PSNR (Peak Signal-to-Noise Ratio) and SSIM (Structural Similarity Index) values, which are referred to as the "Initial PSNR" and "initial SSIM," when comparing the original image with the noisy image. Additionally, it displays the PSNR and SSIM values, which are designated as "PSNR" and "SSIM," respectively, when comparing the original image with the denoised image.

The PSNR value of the filtered image drops as the original image's salt and pepper noise content rises (from 10% to 50%). This shows that when the image's noise level increases, the quality of the filtered image degrades. More noise and poorer image quality are indicative of lower PSNR values.

The SSIM value of the filtered image also drops as the amount of salt and pepper noise in the original image increases.

This shows that as noise levels increase, the structural resemblance between the filtered image and the original, clear image declines. The structural difference is higher when the SSIM values are lower. Filtering is able to improve the image quality to some extent, as evidenced by the higher PSNR and SSIM values for the filtered images compared to the original noisy images.

However, as the noise level becomes more severe (e.g., 50% noise), filtering is less effective in restoring the image to its original quality. This is reflected in the lower PSNR and SSIM values for the highly noisy images.

The decreasing PSNR and SSIM values with increasing noise levels highlight a trade-off between denoising and image quality. Stronger denoising may remove more noise but can also lead to a loss of image detail and structural information, resulting in lower SSIM values.

In summary, these results indicate that filtering can help improve the quality of images corrupted by salt and pepper noise, but the effectiveness of filtering diminishes as the noise level becomes more severe. The choice of the filtering method and its parameters should be carefully considered based on the specific

noise level and the desired trade-off between noise reduction and preserving image details.

TABLE 6: PSNR AND SSIM VALUES FOR LENA.BMP WITH VARYING DENSITY IMAGE

| Image Name |            | Lena           |       |                |      |
|------------|------------|----------------|-------|----------------|------|
|            |            | Initial (PNSR) | PNSR  | Initial (SSIM) | SSIM |
| <b>10</b>  | <b>10</b>  | 15.77          | 28.45 | 0.29           | 0.90 |
| <b>10</b>  | <b>20</b>  | 15.82          | 29.43 | 0.28           | 0.91 |
| <b>10</b>  | <b>40</b>  | 15.75          | 31.02 | 0.26           | 0.92 |
| <b>10</b>  | <b>50</b>  | 15.73          | 30.98 | 0.26           | 0.92 |
| <b>10</b>  | <b>60</b>  | 15.67          | 30.86 | 0.26           | 0.92 |
| <b>10</b>  | <b>70</b>  | 15.62          | 30.73 | 0.26           | 0.92 |
| <b>10</b>  | <b>80</b>  | 15.61          | 29.56 | 0.27           | 0.91 |
| <b>10</b>  | <b>90</b>  | 15.51          | 28.81 | 0.27           | 0.90 |
| <b>10</b>  | <b>100</b> | 15.43          | 28.28 | 0.28           | 0.90 |
| <b>20</b>  | <b>10</b>  | 13.03          | 23.43 | 0.19           | 0.78 |
| <b>20</b>  | <b>20</b>  | 13.03          | 25.33 | 0.17           | 0.85 |
| <b>20</b>  | <b>30</b>  | 12.94          | 26.75 | 0.16           | 0.86 |
| <b>20</b>  | <b>40</b>  | 12.94          | 27.96 | 0.16           | 0.87 |
| <b>20</b>  | <b>50</b>  | 12.87          | 28.45 | 0.15           | 0.89 |
| <b>20</b>  | <b>60</b>  | 12.84          | 27.87 | 0.15           | 0.88 |
| <b>20</b>  | <b>70</b>  | 12.84          | 27.87 | 0.15           | 0.88 |
| <b>20</b>  | <b>80</b>  | 12.77          | 25.77 | 0.16           | 0.83 |
| <b>20</b>  | <b>90</b>  | 12.73          | 23.42 | 0.17           | 0.79 |
| <b>20</b>  | <b>100</b> | 12.69          | 21.63 | 0.18           | 0.75 |
| <b>30</b>  | <b>10</b>  | 11.52          | 19.04 | 0.15           | 0.55 |
| <b>30</b>  | <b>20</b>  | 11.43          | 19.62 | 0.13           | 0.64 |
| <b>30</b>  | <b>30</b>  | 11.39          | 22.33 | 0.12           | 0.71 |
| <b>30</b>  | <b>40</b>  | 11.36          | 23.50 | 0.12           | 0.76 |
| <b>30</b>  | <b>50</b>  | 11.35          | 25.24 | 0.11           | 0.81 |
| <b>30</b>  | <b>60</b>  | 11.29          | 24.79 | 0.11           | 0.80 |
| <b>30</b>  | <b>70</b>  | 11.23          | 22.62 | 0.11           | 0.74 |
| <b>30</b>  | <b>80</b>  | 11.20          | 21.24 | 0.11           | 0.68 |
| <b>30</b>  | <b>90</b>  | 11.13          | 17.95 | 0.12           | 0.57 |
| <b>30</b>  | <b>100</b> | 11.11          | 16.15 | 0.14           | 0.44 |

The result in the table shows that the distribution of salt and pepper (i.e., the ratio of salt to pepper) in the noise affects the quality of the filtered image. When the proportion of salt is higher than that of pepper in the noise, the filtered image tends to have better PSNR and SSIM values compared to when pepper dominates. The PSNR values are generally higher when the proportion of pepper is low (e.g., 10% pepper and 90% salt), indicating better image quality. The SSIM values follow a similar trend, with higher values when pepper is less dominant in the noise distribution.

Filtering is more effective at lower noise levels (e.g., 10% noise) in improving image quality compared to higher noise levels (e.g., 30% noise). Based on the results, an optimal noise distribution for filtering depends on the specific image and application. In many cases, it may be desirable to have a lower proportion of pepper (and a higher proportion of salt) in the noise for better denoising results.

Overall, these results highlight the importance of considering both the noise level and the distribution of salt and pepper when applying filtering techniques to improve image quality. When

the noise increases there is remaining noise on the image as seen on figure 2 and 3.

TABLE 7: PNSR AND SSIM VALUES FOR MONARCH.PNG WITH VARYING DENSITY IMAGE

| Image Name |     | Monarch        |       |                |      |
|------------|-----|----------------|-------|----------------|------|
|            |     | Initial (PNSR) | PNSR  | Initial (SSIM) | SSIM |
| 10         | 5   | 16.78          | 25.01 | 0.33           | 0.93 |
| 10         | 10  | 16.65          | 25.22 | 0.34           | 0.92 |
| 10         | 30  | 16.21          | 26.03 | 0.31           | 0.94 |
| 10         | 40  | 16.00          | 25.94 | 0.31           | 0.94 |
| 10         | 50  | 15.80          | 27.44 | 0.30           | 0.94 |
| 10         | 60  | 15.58          | 26.36 | 0.30           | 0.94 |
| 10         | 70  | 15.35          | 26.24 | 0.29           | 0.94 |
| 10         | 80  | 15.23          | 26.21 | 0.30           | 0.94 |
| 10         | 90  | 15.23          | 26.21 | 0.30           | 0.94 |
| 20         | 10  | 13.90          | 21.91 | 0.23           | 0.81 |
| 20         | 20  | 13.68          | 22.70 | 0.22           | 0.84 |
| 20         | 30  | 13.39          | 24.57 | 0.20           | 0.87 |
| 20         | 40  | 13.18          | 25.15 | 0.20           | 0.87 |
| 20         | 50  | 12.98          | 25.37 | 0.19           | 0.91 |
| 20         | 60  | 12.78          | 25.35 | 0.19           | 0.90 |
| 20         | 70  | 12.62          | 24.80 | 0.20           | 0.89 |
| 20         | 80  | 12.41          | 23.69 | 0.20           | 0.86 |
| 20         | 90  | 12.43          | 21.04 | 0.23           | 0.80 |
| 20         | 100 | 12.07          | 20.00 | 0.21           | 0.79 |
| 30         | 10  | 12.31          | 17.76 | 0.18           | 0.57 |
| 30         | 20  | 12.14          | 20.28 | 0.17           | 0.67 |
| 30         | 30  | 11.92          | 21.41 | 0.16           | 0.74 |
| 30         | 40  | 11.71          | 22.87 | 0.15           | 0.81 |
| 30         | 50  | 11.47          | 23.22 | 0.15           | 0.83 |
| 30         | 60  | 11.32          | 22.81 | 0.15           | 0.82 |
| 30         | 70  | 11.02          | 21.11 | 0.15           | 0.75 |
| 30         | 80  | 10.87          | 19.77 | 0.15           | 0.68 |
| 30         | 90  | 10.68          | 17.86 | 0.16           | 0.58 |

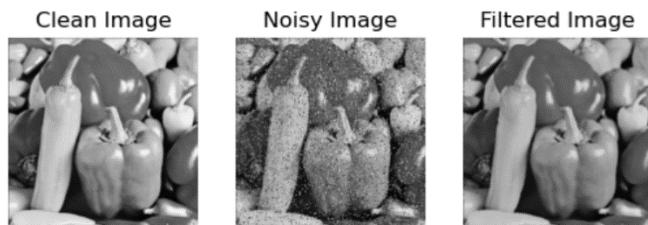


Figure 2: Sample clean, noisy and filtered image with 10% noise out of which 50% is salt and 50% is pepper

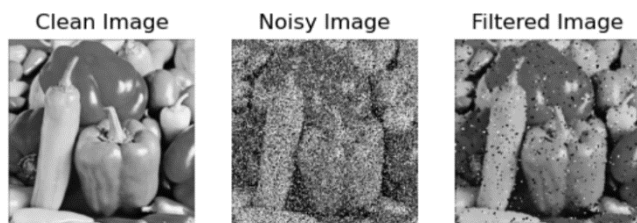


Figure 3: Sample clean, noisy and filtered image with 50% noise out of which 50% is salt and 50% is pepper

## VI. CONCLUSION

This paper introduced an enhanced method for identifying and eliminating salt-and-pepper noise, referred to as the "Improved Connectivity-Based Outlier Factor" (ICOFMED). The method involved two essential parts: Enhancing the noise pixel identification through an improved COF technique, which resulted in a more accurate and precise detection of noisy pixels. Applying a median filter to the identified noisy pixels for the purpose of noise removal. Experimental results exhibited the proposed technique performed good, the PSNR and SSIM values on 'Lena', 'Cameraman', 'Tulips' and 'Pepper'. Although, with increasing salt and pepper noise content in the original image (from 10% to 50%), the PSNR and SSIM value of the filtered image declines. This shows that with increasing noise levels, the filtered image quality deteriorates. These denoising techniques are especially useful in situations where noise is subtle or infrequent, as they help improve image quality and clarity even in noise-free environments. It has great potential across many applications, especially in fields such as high-resolution photography, where maintaining detail fidelity and accuracy remains paramount despite noise. As a result, regardless of the degree of noise density in the images being processed, the continuing development of denoising algorithms can provide substantial benefits.

## VII. RECOMMENDATION

From this work, detection and filtration can be enhanced in a variety of ways for a variety of reasons:

1. The ICOFMed can be improved to increase detection.
2. Other method could be merged with this method to improve detection
3. For filtration other techniques can be used
4. Thresholding in the ICOFMed could further checked

## REFERENCES

- [1] Alghushairy, O., Alsini, R., Soule, T., & Ma, X. (2020). A Review of Local Outlier Factor Algorithms for Outlier Detection in Big Data Streams. *Big Data and Cognitive Computing*, 5(1), 1. <https://doi.org/10.3390/bdcc5010001>
- [2] Chen, F., Huang, M., Ma, Z., Li, Y., & Huang, Q. (2020). An Iterative Weighted-Mean Filter for Removal of High-Density Salt-and-Pepper Noise. *Symmetry*, 12(12), 1990. <https://doi.org/10.3390/sym12121990>
- [3] Chen, J., Zhan, Y., & Cao, H. (2020). Iterative deviation filter for fixed-valued impulse noise removal. *Multimedia Tools and Applications*, 79(33–34), 23695–23710. <https://doi.org/10.1007/s11042-020-09123-x>
- [4] Erkan, U., Thanh, D. N. H., Enginoglu, S., & Memis, S. (2020). Improved Adaptive Weighted Mean Filter for Salt-and-Pepper Noise Removal. *2020 International Conference on Electrical, Communication, and Computer Engineering (ICECCE)*, 1–5. <https://doi.org/10.1109/ICECCE49384.2020.9179351>
- [5] Gao, Z. (2018). An Adaptive Median Filtering of Salt and Pepper Noise based on Local Pixel Distribution. *Proceedings of the 2018 International Conference on Transportation & Logistics, Information & Communication, Smart City (TLICSC 2018)*. *Proceedings of the 2018 International Conference on Transportation & Logistics, Information & Communication, Smart City (TLICSC 2018)*, Chengdu City, China. <https://doi.org/10.2991/tlicsc-18.2018.77>
- [6] Garg, B., & Arya, K. V. (2020). Four stage median-average filter for healing high density salt and pepper noise corrupted images. *Multimedia*

- Tools and Applications, 79(43–44), 32305–32329. <https://doi.org/10.1007/s11042-020-09557-3>
- [7] González-Hidalgo, M., Massanet, S., Mir, A., & Ruiz-Aguilera, D. (2021). Impulsive Noise Removal with an Adaptive Weighted Arithmetic Mean Operator for Any Noise Density. *Applied Sciences*, 11(2), 560. <https://doi.org/10.3390/app11020560>
- [8] Han, J., Kamber, M., Pei, J., & Eecs, S. Z. (2017). Chapter 12 of *Data Mining: Concepts and Techniques*. 25.
- [9] Kaur, K., & Garg, A. (2016). Comparative Study of Outlier Detection Algorithms. *International Journal of Computer Applications*, 147(9), 21–26. <https://doi.org/10.5120/ijca2016911176>
- [10] Liang, H., Li, N., & Zhao, S. (2021b). Salt and Pepper Noise Removal Method Based on a Detail-Aware Filter. *Symmetry*, 13(3), 515. <https://doi.org/10.3390/sym13030515>
- [11] Thanh, D. N. H., Hai, N. H., Prasath, V. B. S., Hieu, L. M., & Tavares, J. M. R. S. (2020). A two-stage filter for high density salt and pepper denoising. *Multimedia Tools and Applications*, 79(29–30), 21013–21035. <https://doi.org/10.1007/s11042-020-08887-6>
- [12] Vasanth, K. (2021). A Decision Based Neighbourhood Referred Asymmetrically Trimmed Modified Trimean for the Removal of High Density Salt and Pepper Noise in Images and Videos. *Wireless Personal Communications*, 120(4), 2585–2609. <https://doi.org/10.1007/s11277-021-08547-4>
- [13] Veerakumar, T., Subudhi, B. N., Esakkirajan, S., & Pradhan, P. K. (2019). Iterative Adaptive Unsymmetric Trimmed Shock Filter for High-Density Salt-and-Pepper Noise Removal. *Circuits, Systems, and Signal Processing*, 38(6), 2630–2652. <https://doi.org/10.1007/s00034-018-0984-4>
- [14] Wang, Z., Bovik, A. C., Sheikh, H. R., & Simoncelli, E. P. (2004). Image Quality Assessment: From Error Visibility to Structural Similarity. *IEEE Transactions on Image Processing*, 13(4), 600–612. <https://doi.org/10.1109/TIP.2003.819861>
- [15] Zhang, H., Zhu, Y., & Zheng, H. (2020). NAMF: A Non-local Adaptive Mean Filter for Salt-and-Pepper Noise Removal (arXiv:1910.07787). arXiv. <http://arxiv.org/abs/1910.07787>
- [16] Zhang, Q., Huang, C., Yang, L., & Yang, Z. (2023). Salt and Pepper Noise Removal Method Based on Graph Signal Reconstruction. 135, 28. <https://doi.org/10.1016/j.dsp.2023.103941>
- [17] Zhou, H., Liu, H., Zhang, Y., & Zhang, Y. (2019). An outlier detection algorithm based on an integrated outlier factor. 16.